Volume 262, number 2, 282–286 FEBS 08272 March 1990

The crystal structure of human muscle aldolase at 3.0 Å resolution

S.J. Gamblin, B. Cooper, J.R. Millar, G.J. Davies, J.A. Littlechild and H.C. Watson

Department of Biochemistry, School of Medical Sciences, University of Bristol, Bristol, UK

Received 4 January 1990; revised version received 29 January 1990

The three-dimensional structure of fructose-1,6-bisphosphate aldolase from human muscle has been determined at 3.0 Å resolution by X-ray crystallography. The active protein is a tetramer of 4 identical subunits each of which is composed of an eight-stranded α/β-barrel structure. The lysine residue responsible for Schiff base formation with the substrate is located near the centre of the barrel in the middle of the sixth β-strand. While the overall topology of the α/β-barrel is very similar to those found in several other enzymes, the distribution of charged residues inside the core of the barrel seems distinct. The quaternary fold of human muscle aldolase uses interfacial regions also involved in the subunit association of other α/β-barrel proteins found in glycolysis, but exploits these regions in a manner not seen previously.

α/β-Barrel; Crystal structure; Isozyme; Schiff base; Type I aldolase; (Human muscle)

1. INTRODUCTION

Fructose-1,6-bisphosphate aldolase (EC 4.1.2.13) is the glycolytic enzyme responsible for catalysing the reversible aldol cleavage of fructose-1,6-bisphosphate into the triose phosphates, D-glyceraldehyde 3-phosphate and dihydroxyacetone phosphate. The active enzyme is a tetramer of 4 identical subunits each with a relative molecular mass of 36000. It is a representative of the class I aldolases which, unlike class II aldolases (for review, see [1]), do not exploit metal ions in the catalytic process. The catalytic cycle of the enzyme involves the formation of a Schiff base intermediate with a lysine residue. The reaction mechanism of class I aldolases has been extensively studied and the aldol cleavage has been shown to proceed by a number of distinct enzyme-substrate intermediates [1]. In mammalian systems there are 3 isozymes, A, B and C, which are expressed in a characteristic pattern [2]. Aldolase A is produced in the developing embryo and several tissues of the adult, most notably in muscle tissue, where it may represent up to 5% of the total cellular protein [3]. The amino acid sequence of human muscle aldolase has been determined [4] and is highly homologous to that of the rabbit muscle enzyme [5]. The low resolution (6 Å) structure of human muscle aldolase [6] and the medium resolution (2.7 Å) structure of the rabbit muscle [7,8] enzyme have been reported. Here we describe the structure determination of human muscle aldolase (ALD) at 3.0 Å resolution.

It is evident from structural studies on both the human and rabbit muscle enzymes that the core of the aldolase subunit is based on a α/β-barrel arrangement. The α/β-barrel structure was first observed in the structure determination of triose phosphate isomerase (TIM) [9]. This folding motif has since been recognised in many systems including the A-domain of pyruvate kinase (PK) [10], KPDG aldolase [11], taka-amylase [12] and glycolate oxidase [13]. The motif is made up of eight α/β supersecondary structure units related by pseudo 8-fold symmetry. Muirhead [14] has made a detailed comparison of several α/β-barrel proteins and has concluded that their overall topologies are very similar even though there is little or no sequence homology between them. Lesk and his colleagues [15] have carried this analysis further by analysing the geometry of several α/β-barrel proteins together with the positioning of side chains associated with the core of each barrel. This work has revealed a simple pattern which elegantly describes the packing of side chains within the barrel. Here we make use of these general observations in the analysis of the structure of this type I aldolase from human muscle.

Correspondence address: H.C. Watson, Department of Biochemistry, School of Medical Sciences, The University, Bristol BS8 1TD, UK

2. EXPERIMENTAL

2.1. *Protein purification and crystallisation*

The protein was extracted from homogenised human leg muscle and purified by ammonium sulphate precipitation and column chromatography procedures according to Scopes [16]. Crystals were prepared for the 3.0 Å data collection by the batch method as already described [6,17]. The protein concentration was approximately 7 mg/ml in 300 mM imidazole, 50 mM KCl, 3 mM Mg acetate, 0.1 mM EDTA at pH 6.5 and ammonium sulphate at 440 g/l. The crystals grow as hexagonal bipyramids and belong to the space group $P6_222$ with $a = b = 96.5$ Å; $c = 167$ Å. Density measurements show that the unit cell contains 3 tetrameric molecules and therefore there is just one monomer in the asymmetric unit. These crystals are similar in habit and unit cell dimensions to those reported earlier for rabbit enzyme [18] but, unlike those crystals, the crystals from human muscle

Published by Elsevier Science Publishers B.V. (Biomedical Division)

are stable to X-ray radiation. A mercuric derivative for use in isomorphous replacement studies was prepared by soaking crystals in 0.1 mM *p*-chloromercuribenzoate (*p*-CMB) for 3 days. A platinum derivative was also prepared by soaking crystals in solutions containing 1 mM K_2PtCl_4 for 16 h prior to irradiation.

2.2. *Data collection and processing*

Diffraction data to 3.0 Å resolution were recorded with an Arndt and Wonacott rotation camera using a sealed tube X-ray source. Three crystals were needed to collect the individual data sets, each of which comprised some 70–80% of the unique diffraction range. The digitised film data were processed using the MOSFLM suite of programs [19]. The native and derivative data sets were of similar quality producing merging statistics (on intensity) close to 7%. The relative changes in structure factor amplitudes between the native and derivative data set were near to 14% in both cases. Patterson maps were calculated in the usual way and the heavy atom positions so determined were refined using both least-squares and different Fourier procedures. The positions and occupancies of the heavy metal binding sites are presented in table 1. When the isomorphous data were used to phase the native structure factors [20] the average figure of merit for those reflexions phased by both derivatives was 0.72.

2.3. *Fourier maps*

The symmetry of space group $P6_222$ means that there are only 4 possible sets of positions at which a tetramer with 222-fold molecular symmetry can be accommodated in the unit cell. Examination of the distribution of electron density at and around each of the possible centres revealed that one of the tetramers must be centered at (1/2, 0, 1/2). With this information it was possible to describe tentative subunit boundaries [6]. Whilst the course of the polypeptide chain could be traced in several regions [17], the map was not of sufficient quality to reveal the overall molecular architecture of the aldolase subunit. In retrospect it is evident that the rather poor quality of the map was due to the fact that only half of the native reflexions were phased by both the mercury and platinum derivatives.

2.4. *Molecular replacement*

As described earlier the amino acid sequence of rabbit muscle aldolase is highly homologous to that of the human muscle enzyme and, as such, the structure of this protein represents a good model for molecular replacement studies on human muscle aldolase. As the coordinates of the published structure of the rabbit muscle enzyme have not been deposited with the Brookhaven Database, the stereographic diagrams contained in the paper describing this work [8] were enlarged and then digitised using a flat bed *x–y* recorder. The two sets of two-dimensional coordinate data were then converted into a three-dimensional coordinate list using a modified version of the program STEREO available from the Brookhaven Data Bank [21]. The resulting C_α coordinates were then used, together with the sequence of the human muscle aldolase [4], to generate an atomic model using the interactive computer graphics program FRODO [22].

The molecular centre information derived from the MIR maps described in section 2.3 limits the number of possible orientations for the aldolase tetramer. The 6 possible arrangements correspond to different alignments of the 3 molecular dyad axes with respect to the crystallographic *a**, *b* and *c* axes. The aldolase tetramer has dimensions of approximately 90 × 90 × 65 Å [6,7] along the molecular axes. Given that 3 tetramers must be accommodated within the unit cell and that the crystallographic *c*-axis is just 167 Å long, it follows that the short dimension of the tetramer must be aligned parallel with the unique axis of the crystal. This leaves just two ways of placing the subunit in the unit cell. The correctness of the starting model was evident from a consideration of the locations of the heavy metal binding sites detailed in table 1. In the correct starting model all 3 methionine residues were within 5 Å of platinum binding sites and cysteine 239 was close to the major mercury binding site.

Table 1

The relative occupancies and the fractional coordinates of the major platinum and mercury binding sites

Derivative		Occupancy	*x*	*y*	*z*
Pt	1	1.0453	0.3567	0.6547	0.0693
	2	0.9044	0.0011	0.4252	0.1623
p-CMB	1	0.9045	0.1754	0.6242	0.9954
	2	0.4741	0.0751	0.8942	0.0739

The unit cell dimensions and the details of the heavy metal compounds used are detailed in the text

3. RESULTS AND DISCUSSION

The initial position of the subunit model was refined by an R-factor search procedure using the programs CADLCF and TSEARCH [19]. Small translation adjustments were made and the starting model was refined by X-ray restrained energy minimisation using the XPLOR package [23]. During the course of 400 cycles of refinement the geometry of the model improved considerably and the agreement residual dropped from 49% to 32% with RMS deviations from ideality of 0.03 Å and 5° for bond lengths and angles, respectively.

3.1. *The subunit model*

The core of the human aldolase structure is made up of alternating β-strands and α-helices as is shown in fig.1. The α/β units are arranged with the helices running approximately antiparallel with the β-strands, so that together the 8 units make up a parallel α/β-barrel with the helices packed around the outside. There are 4 additional helices, 3 of which occur as inserts between the classical strand and helix components making up these particular α/β units. These extra helices are located after β-strands a, b and h. In common with KPDG aldolase, the human muscle aldolase also has an additional N-terminal helix (I in fig.1) which effectively closes off the amino end of the α/β-barrel. There are 6 helices running antiparallel to β-strands which have charged residues at their termini. Of these helices, A2, B2, C, F and G have charged side chains that would form stabilising interactions with the helix dipoles [24]. The cross-section of the barrel is not quite circular but is less eccentric than the α/β-barrel found in TIM [9]. Although the β-strands are generally six or more residues long, only 3 of these can be regarded as forming an integral part of the barrel structure. These 3 residues occur at the same height relative to the barrel axis in all eight strands and they all contribute to a hydrogen bonded net around the barrel. The core of the barrel is made up from 12 residues, two are provided from each of the first, third, fifth and seventh strands while the second, fourth, sixth and eighth strands contribute third, just one amino acid each. These residues are Ala-31, Asp-33, Ile-77, Gly-105, Lys-107, Lys-146, Ile-185, Glu-187, Lys-229, Thr-268, Leu-270 and Ser-300. Of these 12 amino acids, 5 have charged side

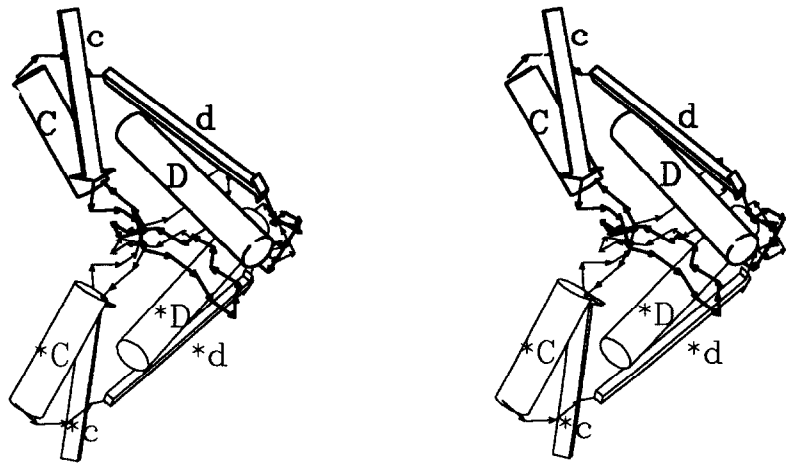

Fig.1. A stereo diagram of a single subunit of human muscle aldolase. The β-strands are shown as arrows and are labelled with lower-case letters, while the α-helices are drawn as cylinders and are labelled in upper-case. The connecting regions between secondary structure units are shown as lines between successive Cα positions with arrowheads indicating the direction of the polypeptide chain. The monomer is orientated so that the readers line of vision is along the molecular two-fold axis which lies parallel to the direction of the crystallographic 6-fold.

chains, this value compares with just two charged residues contributing to the barrel structure of glycolate oxidase and none at all in the case of the TIM barrel [15]. The active site of the enzyme is made up from several of these charged residues as was first pointed out by Sygusch et al. [8]. In contrast the active sites of both TIM and PK occur much more toward the carboxyl ends of the β-strands.

3.2. *Quaternary structure*

The aldolase subunits are packed in a somewhat flattened tetrahedral-like configuration. Each subunit makes significant interactions with just two of its neighbours. The contact regions are largely hydrophobic in nature. The more extensive of the two interfaces is made up by the interaction of side chains from helices E and F from adjacent subunits. These two subunits are related by a dyad axis which lies in the plane approximately perpendicular to the axis of the barrel. The packing arrangement of this subunit interface is shown in fig.2. The relationship between the two subunits is such that the two pairs of symmetry-related helices are approximately antiparallel. Helix E interacts with its symmetry equivalent *E along virtually all its length, while F and *F contact at only their carboxyl ends. Helix E provides the only example in aldolase of a helix with charged side chains at its ends which accentuate the helix dipole. Presumably the antiparallel packing of this helix with its symmetry equivalent will then be additionaly stabilised by electrostatic interactions [24]. The structure of the PK tetramer is such that it also makes a major subunit contact at this edge of the barrel between symmetry-related flanking helices. In the case of PK, however, the dyad axis is positioned such that it runs nearly parallel with the axis of the barrel with the result that the main packing component consists of the almost perpendicular crossing of the 7th flanking helix with its symmetry equivalent [25].

The less extensive subunit interface in the ALD tetramer is formed by both the loop connecting strand c with helix C and the D helix from the two subunits which are related by the second dyad in the plane perpendicular to the barrel axis (as is shown in fig.3). Inspection of the interface of the TIM dimer reveals that both subunits contribute a loop, each of which effectively encircles a methionine residue associated with the other subunit. This loop in TIM joins the third strand and the third helix of the α/β-barrel [9]. The domain structure of PK is arranged so that the second domain occurs as an insertion between the third strand and the third helix of the barrel. These observations concerning the connection within the third α/β unit from these 3 proteins is noteworthy from two viewpoints. Firstly the α/β-barrel motif has pseudo 8-fold symmetry such that none of the 8 ways of superimposing pairs of barrel structures are clearly better than any other [26]. In the cases of TIM, ALD and PK, however, all 3 proteins have subunit/domain interfaces involving the connecting region between the third strand and third helix of the barrel. Secondly, in TIM this loop region plays an essential role in the formation of the active site of the second subunit of the dimer whereas there is no such catalytic role for the corresponding loop in ALD. Indeed it has been shown that monomeric aldolase retains approximately 50% of the catalytic activity of the tetrameric form [27].

The structure reported here for human muscle aldolase is largely similar to that reported for the rabbit muscle enzyme. In the absence of a set of refined coordinates for the rabbit muscle enzyme it is not possible to carry out a detailed analysis of the differences which might exist between the two structures. We have recent-

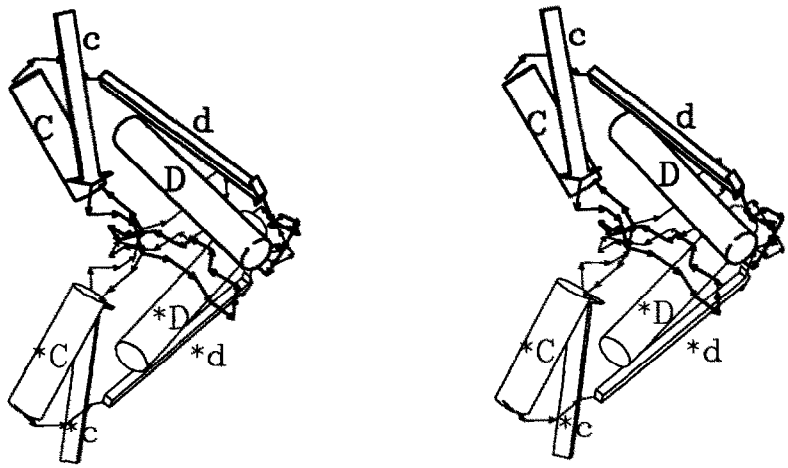

Fig.2. A stereo diagram of the components making up the more extensive of the two dimer interfaces. The subunit which is equivalent to the full monomer shown in fig.1, is drawn in heavier lines than that of its symmetry-related counterpart. Symmetry-related helices are marked with an asterisk. The molecular dyad axis relating the subunits is coincident with the crystallographic a* axis and lies vertically in the plane of the diagram.

ly collected a complete set of diffraction data to a resolution of 2.2 Å from a single crystal of human muscle aldolase using the Daresbury synchroton radiation source. The quality of these data is better than that collected by sealed X-ray source and will greatly facilitate the refinement of the human aldolase structure. It is anticipated that this work, together with results obtained using crystals prepared from protein whose active site lysine has been modified, will help provide detailed information on the catalytic mechanism of the enzyme.

Recently, there has been much interest in the design of specific drugs for the control of parasitic protozoan infections of both domestic animals and humans. In particular the African trypanosomes, which are responsible for causing sleeping sickness, have been studied in some detail [28]. As trypanosomes in the mammalian bloodstream depend entirely on glycolysis for their energy supply, enzymes in this pathway present an obvious target for chemotherapeutic attack. This prospect is enhanced by the fact that these organisms gather many of their glycolytic enzymes into a microbody called a glycosome [29]. Given now the structure of the human muscle aldolase and the sequence of the trypanosome aldolase [30], it may well prove possible to produce drugs designed to specifically inhibit the glycosomal aldolase function.

Coordinates for the human muscle aldolase will be deposited with the Brookhaven protein structure base after refinement of the structure at 2.2 Å resolution. Crystallographic studies on type II aldolases from *Bacillus stearothermophilus* and *Escherichia coli* are also in progress.

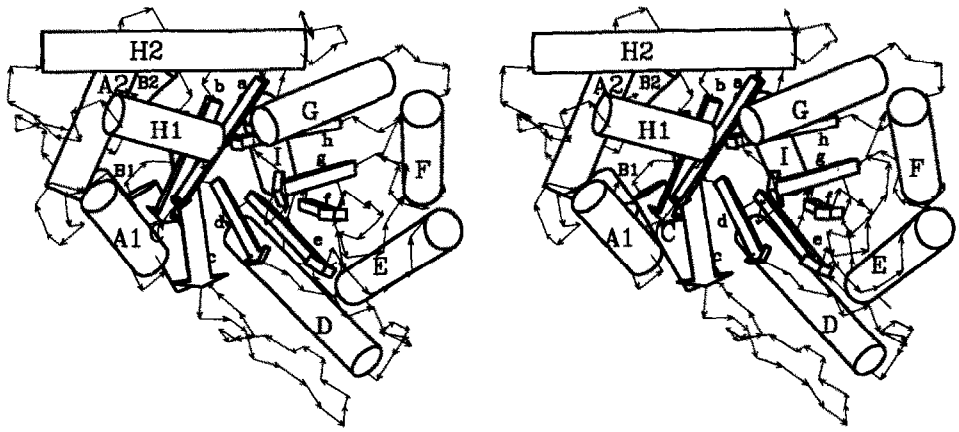

Fig.3. A stereo diagram of the less extensive of the dimer interfaces. The molecular dyad axis relating the two subunits is coincident with the crystallographic b axis and lies horizontally in the plane of the diagram. The figures presented here were prepared using the LESK program (Lesk, A.K. and Hardman, A.D. (1982) Science 216, 539–540).

Acknowledgements: We would like to thank Eleanor Dodson for help with computer programs and Hilary Muirhead for valuable discussions.

REFERENCES

[1] Horecker, B.L., Tsolas, O. and Lai, C.Y. (1975) in: The Enzymes, vol. 7, (Boyer, P.D. ed.) pp. 213–258, Academic, New York.
[2] Penhoet, E.E., Kochman, M. and Rutter, W.J. (1969) Biochemistry 8, 4391–4395.
[3] Lebherz, H.G. and Rutter, W.J. (1969) Biochemistry 8, 109–121.
[4] Izzo, P., Costanzo, P., Lupo, A., Rippa, E., Paolella, G. and Salvatore, F. (1988) Eur. J. Biochem. 174, 569–578.
[5] Tolan, D.R., Amsden, A.B., Putney, S.D., Urdea, M.S. and Penhoet, E.E. (1984) J. Biol. Chem. 259, 1127–1131.
[6] Millar, J.R., Shaw, P.J., Stammers, D.K. and Watson, H.C. (1981) Phil. Trans. Roy. Soc. Lond. B293, 209–214.
[7] Sygusch, J., Boulet, H. and Beaudry, D. (1985) J. Biol. Chem. 260, 15286–15290.
[8] Sygusch, J., Beaudry, D. and Allaire, M. (1987) Proc. Natl. Acad. Sci. USA 84, 7846–7850.
[9] Alber, T., Banner, D.W., Bloomer, A.C., Petsko, G.A., Phillips, D.C., Rivers, P.S. and Wilson, I.A. (1981) Phil. Trans. Roy. Soc. Lond. B293, 159–171.
[10] Stuart, D.I., Levine, M., Muirhead, H. and Stammers, D.K. (1979) J. Mol. Biol. 134, 109–142.
[11] Mavridis, M., Hatada, H., Tulinsky, A. and Lebioda, L. (1982) J. Mol. Biol. 162, 419–444.
[12] Matsuura, Y., Kusunoki, Harada, W., Tanaka, N., Iga, Y., Yasuoka, N., Toda, H., Narita, K. and Kakudo, M. (1980) J. Biochem. 87, 1555–1558.
[13] Lindqvist, Y. and Branden, C.I. (1985) Proc. Natl. Acad. Sci. USA 82, 6855–6859.
[14] Muirhead, H. (1983) Trends Biochem. Sci. 8, 326–329.
[15] Lesk, A.M., Branden, C.I. and Chotia, C. (1985) Proteins 5, 139–148.
[16] Scopes, R.K. (1977) Biochem. J. 161, 253–263.
[17] Millar, J.R. (1983) Ph. D. Thesis Bristol University, Bristol, England.
[18] Heidner, E.G., Weber, B.H. and Eisenberg, D. (1971) Science NY, 171, 3677–679.
[19] SERC Collaborative Computational Projects in Crystallography, Daresbury Laboratory, Daresbury, Warrington, UK.
[20] Blow, D.M. and Rossmann, M.G. (1961) Acta Crystallogr. 14, 1195–1202.
[21] Rossmann, M.G., available from Brookhaven Protein Data Bank, Brookhaven National Laboratory, New York 11973, USA.
[22] Jones, T.A. (1985) Methods Enzymol. 115, 157–171.
[23] Brünger, A.T., Kuriyan, J. and Karplus, M. (1987) Science 235, 458–460.
[24] Hol, W.G.J., Halie, L.M. and Sander, C. (1981) Nature 294, 532–536.
[25] Muirhead, H. (1987) Biological Macromolecules and Assemblies, vol. 3, Active Sites of Enzymes, pp. 145–186.
[26] Lebioda, L., Hatada, M.H., Tulinsky, A. and Mavridis, I. (1982) J. Mol. Biol. 162, 445–458.
[27] Rudolph, R., Westof, E. and Jaenicke, R. (1977) FEBS Lett. 73, 204–206.
[28] Molyneux, D.H. and Ashford, R.W. (1983) The Biology of Trypanosomes and Leishmania, Parasites of Man and Domestic Animals, Taylor and Francis, London.
[29] Opperdoes, F.R. (1985) Br. Med. Bull. 41, 130–136.
[30] Clayton, C.E. (1985) EMBO J. 2, 1721–1728.